Computational Mechanics and Poromechanics for Induced Seismicity and Control

Doctoral Candidate Challenge – ERC INJECT Project

COUPLED THERMO–HYDRAULIC ANALYSIS OF A 2-D GEOTHERMAL RESERVOIR

Presented by:

CHAHID RAHOUTI

Supervised by:

Dr.LOANNIS STEFANOU

June 23, 2025

Contents

1 Problem description

An Enhanced Geothermal System (EGS) is being piloted. Two nearly vertical wells, 500 m apart, intersect a hydraulically stimulated fracture network at a depth of roughly 5 km. Fluids are injected in one well and produced from the other, establishing a forced-convection loop that extracts deep subsurface heat. Although the field layout is three-dimensional, you will model a two-dimensional vertical cross-section that slices through both wells. This simplification retains the essential physics while keeping computational cost modest.
In the absence of solid matrix deformation, the fluid pressure p(x, t) and temperature T (x, t) evolve according to a pair of coupled diffusion equations derived from Biot's porothermoelasticity:

$$\frac{\partial \Delta p}{\partial t} - c_p \nabla^2 \Delta p = \lambda_{pT} \frac{\partial \Delta T}{\partial t} \tag{1}$$

$$\frac{\partial \Delta T}{\partial t} - c_T \nabla^2 \Delta T = \lambda_{Tp} \frac{\partial \Delta p}{\partial t} \tag{2}$$

2 Weak formulation and Implementation

In this section, we will derive the weak formulation of the this couple of equations and then given the geometry associated this problem using GMSH software. We will then implement the weak formulation using the finite element method (FEM) by using a Python implementation.

2.1 Weak formulation

We start by giving the system of equations with boundary conditions:

$$\begin{cases} \dfrac{\partial \Delta p}{\partial t} - c_p \nabla^2 \Delta p = \lambda_{pT} \dfrac{\partial \Delta T}{\partial t}, & x \in \Omega,\ t > 0 \\ \dfrac{\partial \Delta T}{\partial t} - c_T \nabla^2 \Delta T = \lambda_{Tp} \dfrac{\partial \Delta p}{\partial t}, & x \in \Omega,\ t > 0 \\ \Delta p = 2\,\text{MPa}, \quad \Delta T = -130\,^\circ\text{C}, & x \in \Gamma_{\text{inj}},\ t > 0 \\ \Delta p = -1\,\text{MPa}, \quad \mathbf{n} \cdot \nabla \Delta T = 0, & x \in \Gamma_{\text{ext}},\ t > 0 \\ \mathbf{n} \cdot \nabla \Delta p = 0, \quad \mathbf{n} \cdot \nabla \Delta T = 0, & x \in \Gamma_{\text{bord}},\ t > 0 \end{cases} \tag{3}$$

where $\Delta p = p - p_0$ and $\Delta T = T - T_0$ are the pressure and temperature variations. Before starting the weak formulation, we introduce the functional spaces associated with this problem. Due to the mixed boundary conditions, we distinguish two main types of spaces: the solution spaces and the test function spaces.

$$\begin{aligned} S_p &= \left\{ \Delta p \in H^1(\Omega) \;\middle|\; \Delta p = 2\,\text{MPa sur } \Gamma_{\text{inj}},\ \ \Delta p = -1\,\text{MPa sur } \Gamma_{\text{ext}} \right\} \\ S_t &= \left\{ \Delta T \in H^1(\Omega) \;\middle|\; \Delta T = -130\,^\circ\text{C sur } \Gamma_{\text{inj}} \right\} \end{aligned} \tag{4}$$

$$\begin{aligned} V_p &= \{u \in H^1(\Omega),\ u = 0 \text{ on } \Gamma_{\text{inj}} \cup \Gamma_{\text{ext}}\} \\ V_t &= \{v \in H^1(\Omega),\ v = 0 \text{ on } \Gamma_{\text{inj}}\} \end{aligned} \tag{5}$$

Then, let $u \in V_p$ and $v \in V_t$ be the test functions, so, by Green's theorem and integration by parts we can write the weak formulation of the problem as follows:

$$\begin{cases} \displaystyle\int_\Omega \frac{\partial \Delta p}{\partial t} u\,dx + c_p \int_\Omega \nabla \Delta p \cdot \nabla u\,dx - c_p \int_{\Gamma_{\text{inj}} \cup \Gamma_{\text{ext}} \cup \Gamma_{\text{bord}}} (\nabla \Delta p \cdot n) u\,dx = \lambda_{pT} \int_\Omega \frac{\partial \Delta T}{\partial t} u\,dx, \quad \forall u \in V_p \\ \displaystyle\int_\Omega \frac{\partial \Delta T}{\partial t} v\,dx + c_T \int_\Omega \nabla \Delta T \cdot \nabla v\,dx - c_T \int_{\Gamma_{\text{inj}} \cup \Gamma_{\text{ext}} \cup \Gamma_{\text{bord}}} (\nabla \Delta T \cdot n) v\,dx = \lambda_{Tp} \int_\Omega \frac{\partial \Delta p}{\partial t} v\,dx, \quad \forall v \in V_t \end{cases} \tag{6}$$

After sampling this weak formulation by the bord conditions, we can write the weak formulation as follows:

$$\begin{cases} \displaystyle\int_\Omega \frac{\partial\,\Delta p}{\partial t} u\,dx + c_p \int_\Omega \nabla \Delta p \cdot \nabla u\,dx = \lambda_{pT} \int_\Omega \frac{\partial\,\Delta T}{\partial t} u\,dx, \quad \forall u \in V_p \\ \displaystyle\int_\Omega \frac{\partial\,\Delta T}{\partial t} v\,dx + c_T \int_\Omega \nabla \Delta T \cdot \nabla v\,dx = \lambda_{Tp} \int_\Omega \frac{\partial\,\Delta p}{\partial t} v\,dx, \quad \forall v \in V_t \end{cases} \tag{7}$$

These two forms are bilinear (thanks to the linearity of the integral), continuous (due to the continuous embedding of H^1 into L^2), and coercive (thanks to the Poincaré inequality). Therefore, we can use the Lax-Milgram theorem to prove the existence and uniqueness of the solution to this problem.
Find $(\Delta p, \Delta T) \in S_p \times S_t$ such that:

$$\begin{cases} \displaystyle\int_\Omega \frac{\partial\,\Delta p}{\partial t} u\,dx + c_p \int_\Omega \nabla \Delta p \cdot \nabla u\,dx = \lambda_{pT} \int_\Omega \frac{\partial\,\Delta T}{\partial t} u\,dx, \quad \forall u \in V_p \\ \displaystyle\int_\Omega \frac{\partial\,\Delta T}{\partial t} v\,dx + c_T \int_\Omega \nabla \Delta T \cdot \nabla v\,dx = \lambda_{Tp} \int_\Omega \frac{\partial\,\Delta p}{\partial t} v\,dx, \quad \forall v \in V_t \end{cases} \tag{8}$$

Now, we giving the matrix form of the weak formulation, we can write the system as follows:

$$\begin{cases} M_p \dot{\Delta p} + K_p \Delta p = \lambda_{pT} M_p t \Delta T \\ M_t \dot{\Delta T} + K_t \Delta T = \lambda_{Tp} M_p \Delta p \end{cases} \tag{9}$$

where M_p and M_t are the mass matrices, and K_p and K_t are the stiffness matrices associated with the pressure and temperature equations, respectively. The terms λ_{pT} and λ_{Tp} are coupling coefficients between the pressure and temperature equations. I will use Euler backward method and theta method to solve this system of equations.

2.2 Geometry and mesh generation

The geometry of the problem is a 2D vertical cross-section of the geothermal reservoir, which can be represented as a rectangle with two wells. The left well is the injection well, and the right well is the production well.

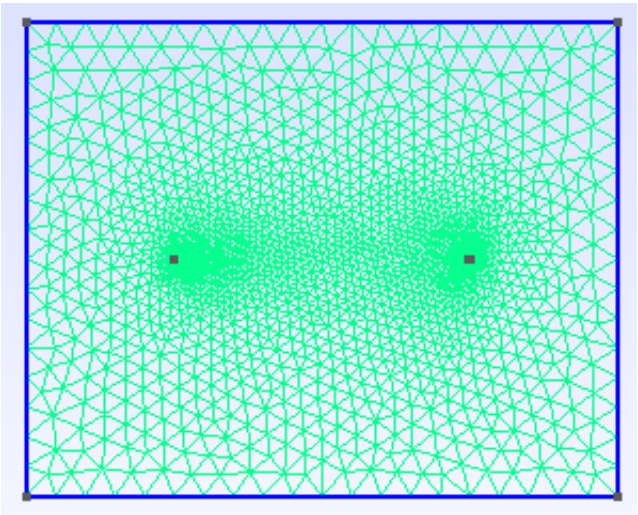

Figure 1: Geometry with wells as circles

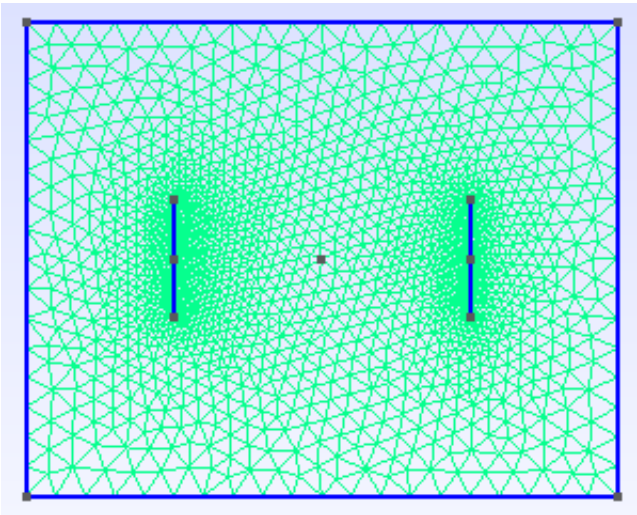

Figure 2: Geometry with wells as segments

2.3 Implementation and Results

The implementation of this system of equations is done using the finite element method (FEM) in Python. To respect the units used in the computations, I performed some conversions, such as from Celsius to Kelvin and for the initial condition we have the reservoir is at equilibrium it means that 10. You can find the code in the link of the GitHub repository. https://github.com/chahid-rahouti/Coupled-Thermo-Hydraulic

$$\Delta p(0,x) = p(0,x) - p_0(0,x) = 0 \quad \text{et} \quad \Delta T(0,x) = T(0,x) - T_0(0,x) = 0 \tag{10}$$

The results show the evolution of the pressure and temperature in the geothermal reservoir over

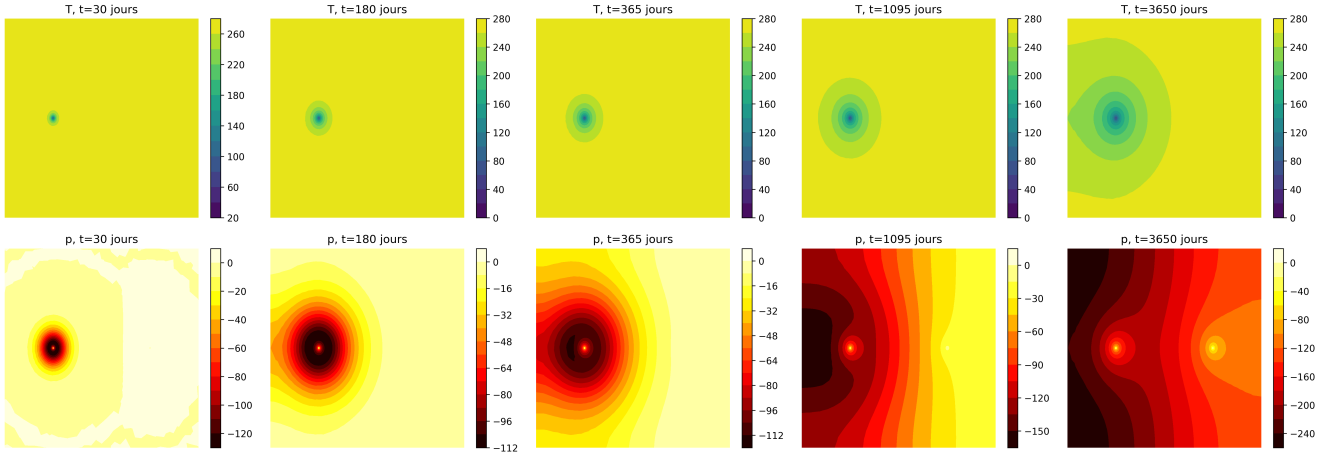

Figure 3: Solution of the coupled system of equations for pressure and temperature over time (30 days, 6 mouths, 1 year, 3 years, 10 years)

time. The pressure increases in the injection well and decreases in the production well, while the temperature decreases in the injection well and increases in the production well. This behavior is consistent with the expected physics of a geothermal reservoir.(see Figure 3) I know that the results are not very good, because in the many references i find the distibution of the pressure and temperature are go to the injection wells to the production wells, but in my case the pressure and temperature are not going to the production well. I think there is a problem but at this moment I don't know what is the problem. You can see this references ([1], [2], [3], [4], [5], [6]).

3 Conceptual Fault Extension

In this section, we will extend the conceptual fault model to include the effects of faults on the pressure and temperature distribution in the geothermal reservoir. The conceptual fault model is based on the assumption that the faults are permeable and can allow fluid flow between the reservoir and the fault.

3.1 Fault model

We are modeling the faults as a surface of discontinuity and jump in the pressure and temperature distribution in the reservoir 4. In our case, we can add this surface of discontinuity at our geometry, and we can use the same weak formulation as before, but we need to add the effects of the faults. To solve the system in this case, we will use the discontinuous Galerkin method (DGM). The DGM is a numerical method take into account the discontinuities in the solution. In this case, we

can write the weak formulation of the system with the faults as follows:

$$\begin{cases} \displaystyle\int_\Omega \frac{\partial\,\Delta p}{\partial t} u\,dx + c_p \int_\Omega \nabla \Delta p \cdot \nabla u\,dx + \int_{\Gamma_{\text{fault}}} \kappa_p [\Delta p] u\,ds = \lambda_{pT} \int_\Omega \frac{\partial\,\Delta T}{\partial t} u\,dx, & \forall u \in V_p \\ \displaystyle\int_\Omega \frac{\partial\,\Delta T}{\partial t} v\,dx + c_T \int_\Omega \nabla \Delta T \cdot \nabla v\,dx + \int_{\Gamma_{\text{fault}}} \kappa_T [\Delta T] v\,ds = \lambda_{Tp} \int_\Omega \frac{\partial\,\Delta p}{\partial t} v\,dx, & \forall v \in V_t \end{cases} \tag{11}$$

where $[\Delta p]$ and $[\Delta T]$ are the jumps in the pressure and temperature across the fault surface Γ_{fault}, when κ_p and κ_T are the fault permeabilities. The jumps are defined as the difference between the values of the pressure and temperature on either side of the fault:

$$[\Delta p] = \Delta p^+ - \Delta p^- \quad \text{et} \quad [\Delta T] = \Delta T^+ - \Delta T^- \tag{12}$$

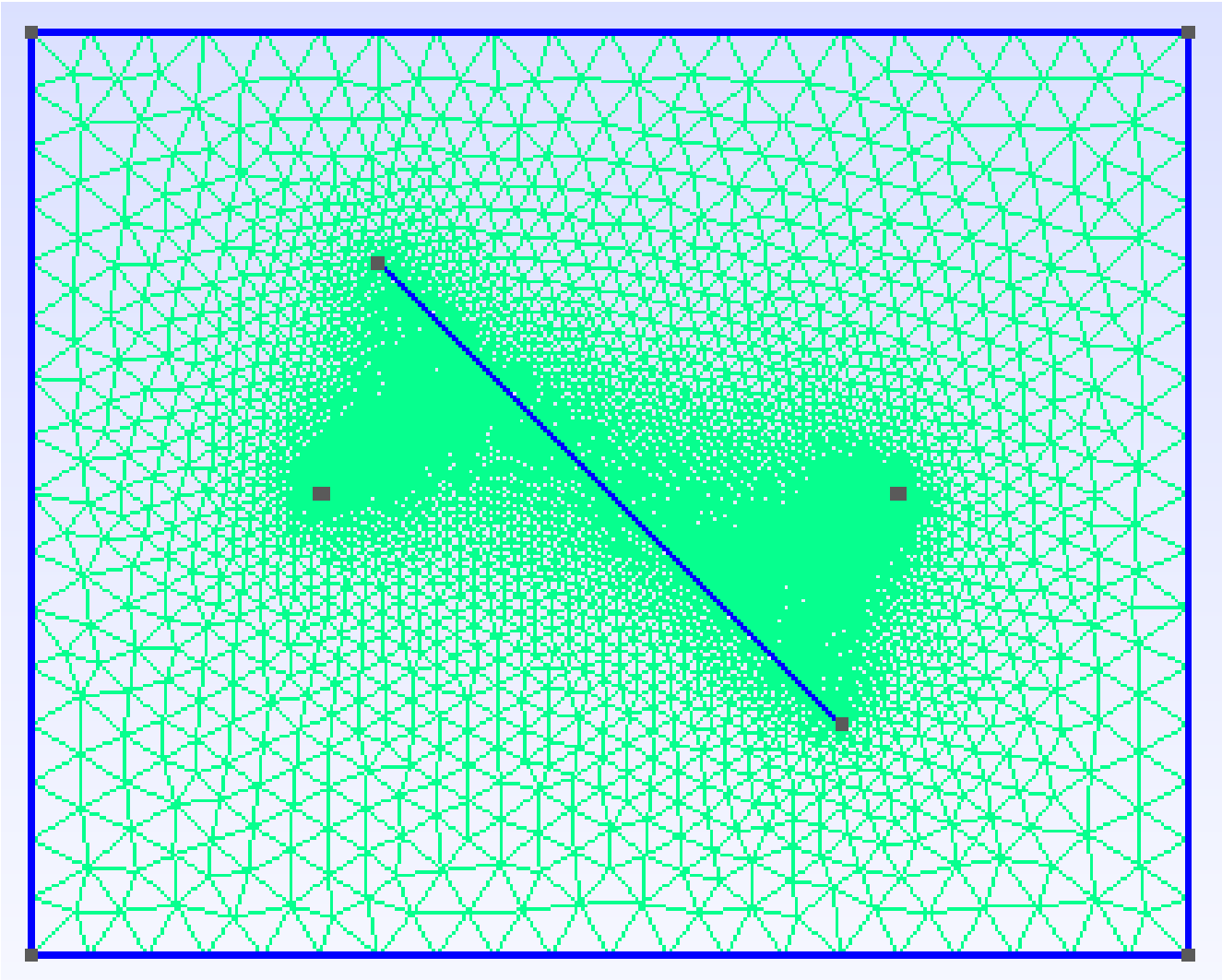

Figure 4: 2D conceptual fault model

3.2 Impact of the fault on the reservoir

- **Pressure redistribution:** Permeable faults (low κ_p the fault resistance) can reduce the drawdown by redistributing pressure to zones of lower permeability. It means, approximately a $\sim 30\%$ reduction in the pressure gradient between the injection and production wells ([7], [8]).

- **Thermal breakthrough:** The fault acts as a preferential pathway for the injected cold water. If κ_T is low, the breakthrough time is inversely proportional to $t_{\text{breakthrough}} \propto \frac{1}{\kappa_T}$ (reduction up to 50%). There is a risk of premature cooling of the production well ([9], [12]).
- **Advantage:** Increased production rate (up to +20%) due to the connection of permeable zones.
- **Risk:** If κ_p is too high, the fault may drain the injected fluid towards the exterior, reducing thermal recovery.

4 Closed-Loop Control Challenge

4.1 Mathematical problem

In this situation, we search how we can control the temperature difference between the injection and production wells, or exactly maximize the duration when $\Delta T_{\text{ext}}(t) \geq \Delta T_{\min}$ for all $t \in [0,\, 10\,\text{ans}]$. So, the injection flow rate $Q_{\text{inj}}(t)$ (or $\Delta p_{\text{inj}}(t)$) becomes a control variable of the problem. we can use the optimal control theory to solve this problem. We formulate a constrained optimization problem:

$$\min_{Q_{\text{inj}}(t)} \underbrace{\int_0^{10\,\text{years}} L(\Delta T_{\text{ext}}(t), Q_{\text{inj}}(t))\, dt}_{\text{Total control cost}} \qquad \text{such that } \Delta T_{\text{ext}}(t) \geq \Delta T_{\min} \quad \forall t \in [0,\, 10\,\text{years}] \tag{13}$$

The function $L(\Delta T_{\text{ext}}(t), Q_{\text{inj}}(t))$ is generally of the form:

$$L(\Delta T_{\text{ext}}(t), Q_{\text{inj}}(t)) = \underbrace{\beta_1 [\Delta T_{\min} - \Delta T_{\text{ext}}(t)]_+^2}_{\text{Penalty if } \Delta T_{\text{ext}} < \Delta T_{\min}} + \underbrace{\beta_2 Q_{\text{inj}}^2}_{\text{Pumping consumption}} \tag{14}$$

where $[x]_+ = \max(0, x)$ and β_1, β_2 are positive constants.

4.2 Proposed Strategy

Adaptive control: Adjust Q_{inj} in real time using a PI-type control law based on the error $e(t) = \Delta T_{\text{ext}}(t) - \Delta T_{\min}$:

$$Q_{\text{inj}}(t) = K_p\, e(t) + K_i \int_0^t e(\tau)\, d\tau, \tag{15}$$

where K_p and K_i are tuned by prior modeling.

Operational limits: $Q_{\min} \leq Q_{\text{inj}} \leq Q_{\max}$ to avoid fracturing or critical pressure drop.

We can also use deep learning methods or data assimilation to control the system more effectively. For further information, see [13]. There are other methods such as closed-loop optimization of geothermal reservoir production using $Q_{\text{inj}}(t)$ like a variable of optimization, see ([14], [15]).

Bibliography

[1] Yuting Luo, Juyan Wei, Meilong Fu, Li Fang, and Xudong L.
Analysis of Enhanced Geothermal System Reservoir Parameters and Fractures on Heat Recovery Efficiency Based on a Single-Phase Conduction Model.
Article.

[2] Wang Jiwei, Ming Chen, Bo Zhang, et al.
Numerical Simulation of Hydraulic Fracturing Damage Evolution in Geothermal Reservoirs with Natural Fractures Based on THMD Coupling Model.
Conference Paper, June 2022.
DOI: 10.56952/ARMA-2022-0951.
Available at: `https://www.researchgate.net/publication/364247123`

[3] Yifan Fan, Shikuan Zhang, Yonghui Huang, Zhonghe Pang, and Hongyan Li.
Determining the Recoverable Geothermal Resources Using a Numerical Thermo-Hydraulic Coupled Modeling in Geothermal Reservoirs.
Frontiers in Earth Science, 2022.
Available at: `https://www.frontiersin.org/articles/10.3389/feart.2022.XXXXXX`

[4] Hua-Peng Chen and Musa D. Aliyu.
Numerical modelling of coupled thermo-hydraulic problems for long-term geothermal reservoir productivity.
VII International Conference on Computational Methods for Coupled Problems in Science and Engineering (COUPLED PROBLEMS 2017),
M. Papadrakakis, E. Oñate and B. Schrefler (Eds), 2017.
Department of Engineering Science, University of Greenwich, UK.

[5] Musa D. Aliyu and Hua-Peng Chen.
Numerical modelling of coupled hydro-thermal processes of the Soultz heterogeneous geothermal system.
ECCOMAS Congress 2016, VII European Congress on Computational Methods in Applied Sciences and Engineering,
M. Papadrakakis, V. Papadopoulos, G. Stefanou, V. Plevris (eds.), Crete Island, Greece, 5–10 June 2016.
Department of Engineering Science, University of Greenwich, UK.

[6] S. N. Pandey and Vikram Vishal.
Sensitivity analysis of coupled processes and parameters on the performance of enhanced geothermal systems.
Scientific Reports, 7:17057, 2017.
DOI: 10.1038/s41598-017-14273-4.
Available at: `https://www.nature.com/articles/s41598-017-14273-4`

[7] Alexandros Daniilidis, Sanaz Saeid, Nima Gholizadeh Doonechaly.
The fault plane as the main fluid pathway: Geothermal field development options under subsurface and operational uncertainty.

Geothermics, Volume 85, 2020, 101771.
Delft University of Technology, University of Geneva, ETH Zurich.
DOI: 10.1016/j.geothermics.2019.101771.
Available at: https://www.sciencedirect.com/science/article/pii/S0375650519303372

[8] Kingsley Anyim, Quan Gan.
Fault zone exploitation in geothermal reservoirs: Production optimization, permeability evolution and induced seismicity.
Geothermics, Volume 111, 2024, 102899.
DOI: 10.1016/j.geothermics.2023.102899.
Available at: https://www.sciencedirect.com/science/article/pii/S0375650523001842

[9] Caroline Zaal, Alexandros Daniilidis, Femke C. Vossepoel.
Economic and fault stability analysis of geothermal field development in direct-use hydrothermal reservoirs.
Geothermal Energy, 2022.
DOI: 10.1186/s40517-022-00237-5.
Available at: https://geothermal-energy-journal.springeropen.com/articles/10.1186/s40517-022-00237-5

[10] Charbel Salameh, Patrick Schalbart, Bruno Peuportier.
Optimal Control Strategies for Energy Production Systems using Buildings Thermal Mass.

[11] Zhihong Lei, Yulong Zhang, Qiliang Cui, Yu Shi.
The injection-production performance of an enhanced geothermal system considering fracture network complexity and thermo-hydro-mechanical coupling in numerical simulations.
Scientific Reports, 2023.
Available at: https://www.nature.com/articles/s41598-023-31913-6

[12] Robert Egert, Maziar Gholami Korzani, Sebastian Held, Thomas Kohl.
Thermo-hydraulic Modeling of an Enhanced Geothermal System in the Upper Rhine Graben using MOOSE/TIGER.
Karlsruhe Institute of Technology, Institute of Applied Geosciences, Division of Geothermal Research.
Robert.Egert@kit.edu

[13] Nanzhe Wang, Haibin Chang, Xiangzhao Kong, Martin O. Saar, Dongxiao Zhang.
Deep learning based closed-loop optimization of geothermal reservoir production.

[14] Yaroslav V. Vasyliv, Gabriela A. Bran-Anleu, Alec Kucala, Sam Subia, Mario J. Martinez.
Analysis and Optimization of a Closed Loop Geothermal System in Hot Rock Reservoirs.
Sandia National Laboratories, Albuquerque, NM.

[15] Wanju Yuan, Zhuoheng Chen, Stephen E. Grasby, Edward Little.
Closed-loop geothermal energy recovery from deep high enthalpy systems.